COMMUNICATION

Low-dimensional Iodide Perovskite Nanocrystals Enables Efficient Red Emission

Laura Martínez-Sarti,[a] Seung Hyeon Jo,[b] Young-Hoon Kim,[b] Michele Sessolo,[a] Francisco Palazon,[a,*] Tae-Woo Lee[b] and Henk J. Bolink.[a]

We report herein a simple ligand-assisted reprecipitation method at room temperature to synthesize mixed-cation hybrid organic-inorganic perovskite nanocrystals with low structural dimensionality. The emission wavelength of iodide-based perovskites is thus tuned from the near-infrared to the red part of the visible spectrum. While this is mostly achieved in literature by addition of bromide, we demonstrate here a controllable blueshift of the bandgap by varying the chain length of the alkylammonium ligands. Furthermore, an antisolvent washing step was found to be crucial to purify the samples and obtain single-peak photoluminescence with narrow linewidth. The so-formed nanocrystals exhibit high and stable photoluminescence quantum yields exceeding 90% over 500 hours, making these ideal materials for light-emitting applications.

Metal halide perovskites have emerged in the last years as promising materials for applications in optoelectronic devices such as solar cells,[1–3] light-emitting diodes (LEDs)[4–8] or X-ray detectors.[9,10] The reason behind the interest for perovskite nanocrystals (NCs) is based on their high photoluminescence quantum yield (PLQY), related to the spatial charge carrier confinement and passivation of surface states by organic capping ligands, as well as the narrower emission lines and higher stabilities as compared to their bulk counterparts.[11–15] Considering the simple methods that have been developed for their synthesis, perovskite NCs have become ideal materials for electroluminescent and phosphors applications.

Although seminal reports focused on hybrid methylammonium lead halide perovskites,[16] several recent studies have shown that the introduction of inorganic Cs+ cations in small quantities (≤20%) into these hybrid materials leads to beneficial effects

including an enhanced stability and reproducibility.[17–19] It is well known that the shape, size and optical properties of perovskite NCs are strongly affected by the ligands.[20–27] When the nanocrystals' size is less or equal to the exciton Bohr diameter, they exhibit quantum confinement, and the optical absorption and photoluminescence (PL) are blue-shifted compared to the bulk counterpart. It has been reported that the dimensionality of the NCs can be modulated by varying the alkyl chain length and/or the concentration of the surface ligands, and consequently, tune the emission features.[21,24] Fundamentally, this is linked to the fact that the ammonium head group of alkylammonium ligands can occupy the A-site in the $APbX_3$ perovskite structure. As a result, using long ammonium (LA) molecules in combination with a small A-cation such as methylammonium ($CH_3NH_3^+$, MA), formamidinium ($CH(NH_2)_2^+$, FA) or Cs+ may lead to the so-called Ruddlesden-Popper quasi-2D phase,[28,29] with the generic formula $(LA)_2(A)_{n-1}Pb_nI_{3n+1}$, where perovskite slabs of n layers are separated by a bilayer of the large ammonium cation. These quasi-2D structures show quantum confinement effects strongly related to the n-value,[21,30] which in turn can be tuned by the amount and length of the alkyl chain used in the synthesis. More precisely, the thickness of a single lead iodide perovskite monolayer is approximately 6.3 Å, corresponding to twice the length of the Pb-I bond, or in other words to the height of a PbI_6 octahedron (octahedral tilting and slight differences in Pb-I bond lengths are neglected in this approximation).[29] In contrast, reported values for the exciton Bohr diameter of $MAPbI_3$ are around 2.2nm[31] to 4.6nm.[32] Therefore, quasi-2D $(LA)_2(MA)_{n-1}Pb_nI_{3n+1}$ start showing quantum-confinement effects when the n value is roughly below 10 (corresponding to a layer thickness of around 6.3 nm, hence comparable with the exciton Bohr diameter). Above a value of ca. 10, n can be considered large enough so that the quasi-2D crystal is equivalent to a 3D MAPbI3 structure (n=∞).[29] As has recently been shown, these quantum-confined quasi-2D perovskites (with n<10) are ideal materials for efficient perovskite LEDs.[5]

a. Instituto de Ciencia Molecular (ICMol), Universidad de Valencia, Catedrático José Beltrán, 2, 46980 Paterna, Spain
b. Department of Materials Science and Engineering, Institute of Engineering Research, Research Institute of Advanced Materials, Nano Systems Institute (NSI), BK21 PLUS SNU Materials Division for Educating Creative Global Leaders, Seoul National University, 1 Gwanak-ro, Gwanak-gu, Seoul 08826, Republic of Korea

In this work, we describe a simple ligand-assisted reprecipitation (LARP) method at room temperature (RT) to prepare efficient red-emitting low-dimensional NCs and study the change in the optical properties as a function of different synthesis conditions. In particular, we will discuss the variation of the bandgap from the near-infrared (NIR) to the visible range as a function of the alkylammonium molecule length. Mixed-cation MA-Cs perovskite NCs were prepared by a direct, non-template method synthesis based on a previously published protocol[33] with slightly modified conditions and starting materials. Briefly, a solution of PbI_2 (dissolved in 1-octadecene, ODE, with oleylamine, oleylA, and oleic acid, OA, ligands) was injected at RT in a solution of MAI and CsI (0.8:0.2 ratio; dissolved in a mixture of 1-butanol, 1-BuOH, and ODE with OA) leading to the formation of the perovskite NCs, which were subsequently washed by centrifugation steps (see experimental section for more details). The optical characteristics of the obtained NCs are presented in Fig. 2a. An absorption onset around 740 nm with the corresponding photoluminescence peak centred at 747 nm (FWHM of 45 nm), together with a sharp absorption feature at 617 nm and its Stokes-shifted PL peak centred at 625 nm (FWHM of about 30 nm), can be observed. It is worth noting that when the synthesis is carried out at 0 °C instead of RT, no significant spectral differences are observed, whereas at high temperature a rather clear yellow solution with very low PL is obtained (Fig. S1, ESI†). Hence, all further syntheses were carried out at RT. The two aforementioned features observed in the optical characterization of the sample (Fig. 2a) are consistent with 3D (narrow bandgap) and quasi-2D (wide bandgap due to quantum confinement) iodide perovskite NCs.[21,34] We note that this is not the first report on quantum confined perovskite structures using oleylamine. Almeida et al. have shown that oleylammonium cations can induce anisotropic growth,[35] while others have claimed that oleylammonium (despite the length of its backbone and its non-planar configuration caused by the

vinyl bond) may lead to quasi-2D structures.[36,37] In order to further prove this hypothesis, we conducted XRD analysis (Fig. 2b) on drop-casted NCs films. The broad diffraction peaks centred at 2Θ = 14.0° and 2Θ = 28.3° are consistent with the formation of 3D iodide perovskite NCs. In addition, sharp peaks at low angles (i.e., larger interatomic distances) are clearly visible, confirming the presence of quasi-2D crystals consisting of perovskite sheets separated by long-chain oleylammonium cations. In principle, it is possible to determine the n value of quasi-2D Ruddlesden-Popper crystals with chemical formula $(LA)_2(A)_{n-1}Pb_nI_{3n+1}$ by XRD. Nonetheless, this requires high quality data up to very low diffraction angles,[29,38] which we were not able to acquire here. Moreover, the XRD peaks' positions and spacing do not depend only on the n value but also on the length of the LA molecule, so that our data cannot be directly compared with that of Ruddlesden-Popper crystals obtained with other LA molecules such as butylammonium.[29] However, based on PL characterization, it is reasonable to assume a value of n=4 for the emission centered at 625nm.[39] It is worth noting that pure 2D (n=1) lead iodide perovskites exhibit an emission peak around 525 nm.[39,40] Hence the formation of pure 2D crystals can be excluded. TEM characterization (Fig. 2c) revealed the presence of cubic-shaped perovskite nanocrystals with a typical dimension of 10 nm. This is consistent with the broad peaks in XRD as well as the low-energy optical transitions previously discussed for 3D NCs. Additionally, TEM analysis also showed large nanosheets without a well-defined morphology, similar to previous observations of quasi-2D oleylammonium lead halide perovskites,[36] confirming the coexistence of both 3D and quasi-2D iodide nanocrystals.

While the iodide perovskite NCs discussed so far emit preferentially in the NIR, the PL can be blue-shifted through a reduction of the material structural dimensionality, i.e. the number of lead halide layers separated by alkylammonium in the quasi-2D structure. Several reports have shown that the inorganic layer thickness can be tuned by the amount and length of the alkylammonium ligands.[23,30,41–43] Hereafter we controlled the PL maximum by replacing oleylA ligands by smaller saturated alkylamines with decreasing chain lengths: decylamine (decylA), octylamine (octylA) and hexylamine (hexylA). All other synthesis conditions, in particular the concentration of alkylamine (thus also the amine/acid ratio), were unvaried. In all cases, the synthesis led to the formation of nanocrystals. The colloidal dispersions in toluene exhibited PL with maxima centred at 697 nm, 676 nm and 655 nm for decylA, octylA and hexylA, respectively (Fig. 2d). Hence a decrease of the alkyl chain length of the ligand led to a progressive blue-shift of the PL maximum. This trend was also observed by other groups,[20,24,44] and some attributed it to the faster diffusion of shorter chain ammonium ions which result in faster on– off exchange rates. It is important to note that shorter amines not only lead to a reduction of the space between the 3D "slabs" in the quasi-2D structure, directly linked to the alkyl chain length. The easier intercalation of the shorter amines results in stabilization of thinner 3D layers (i.e., lower n-values) leading to exciton confinement and hence PL blue-shift. Additionally, the
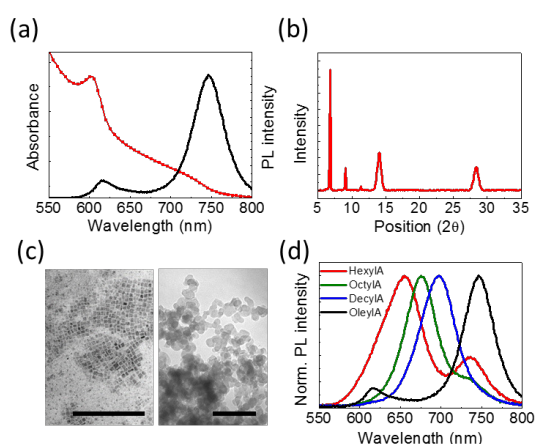

Fig. 2 (a) Absorbance (red line) and PL spectra (black line), (b) X-ray diffraction pattern and (c) TEM images (scale bar is 200 nm) of the mixed Cs-MA perovskite nanostructures obtained using oleylamine as ligand. The images illustrate the formation of 3D (left) and quasi-2D structures (right). (d) Comparison of the PL spectra registered for NCs obtained with different alkyl chain length ligands.
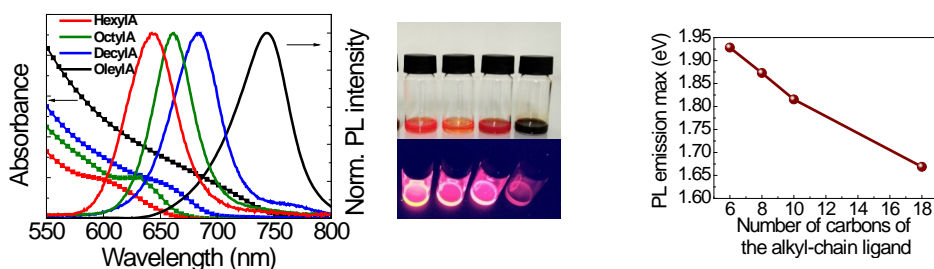
Fig. 3 (a) Absorbance (square symbols with lines) and PL (lines) for further purified samples (with 1-BuOH) obtained using different ligands during the synthesis. On the right, photographs of colloidal solutions under ambient light (top) and under UV excitation (λ = 365 nm) (bottom) for hexylA (H-B), octylA (O-B), decylA (D-B) and oleylA (A-B). (b) Energy at the PL maximum as a function of the number of carbon atoms in the capping ligand.

use of shorter amines results in an enhancement of the PLQY compared to the oleylA sample (28%), reaching values of 90%, 85% and 68% for decylA, octylA and hexylA, respectively. However, as in the original synthesis with oleylA, most PL spectra present broad and multiple peaks, which points out the coexistence of different species (different n-values).

In order to purify the samples, we tested the addition of 1-BuOH in large quantities during the first centrifugation step (see experimental section for more details). The use of additional solvents during the purification step has been reported to change the optical properties of the synthesized product.[45] Upon this treatment, the resulting NCs dispersions showed a main PL peak centred at 743 nm, 683 nm, 662 nm and 643 nm for the oleylA, decylA, octylA and hexylA ligand, respectively (Fig. 3a). Based on literature, these PL bands can be ascribed to quasi-2D lead iodide NCs with n = ∞ (3D), n = 7, n = 6, and n= 5, respectively.[39] As can be seen by comparing Fig. 3a and Fig. 2d, this modified washing step leads to more symmetric PL spectra that suggest a smaller distribution of species in the suspension. Representative TEM images of samples synthesized with short amines and washed with butanol are presented in Fig. S2. Additionally, we observed a small blue-shift of the main PL signal between the pristine samples and the samples washed with 1-BuOH (Fig. S3, ESI†). Also worth to note is the steady change of the PL maximum of the treated samples as a function of the size of the alkyl chain ligand, represented in Fig. 3b. Decreasing the length of the capping ligand from oleylA to decylA results in a PL emission shift of about 147 meV, which

further shifts by 58 meV and 55 meV from decylA to octylA and from octylA to hexylA, respectively. The associated PLQYs for the further purified NCs were 24%, 87%, 91% and 82% for oleylA, decylA, octylA and hexylA, respectively. Remarkably, the use of 1-BuOH during the purification process induced a PLQY enhancement in the hexylA sample, while oleylA, decylA and octylA PLQYs remained almost unvaried.

On these further purified samples, we also observed the characteristic sharp peaks at low angles in the diffraction patterns (Fig. 4a) (see Figure S4 for complete X-ray diffraction patterns). As expected from the change in the alkyl chain length, these peaks are also shifted. Indeed, the interlayer spacing increases linearly with increasing the alkyl chain length, in agreement with previous reports.[43,46] The formation of quasi-2D crystals with different periodicities as a function of alkyl chain length, as evidenced by XRD, is consistent with the progressive blue-shift of the optical characteristics presented in Fig. 3a, as a result of quantum confinement.[21,47]

In order to evaluate the stability of the materials, the nanocrystals were kept dispersed in toluene, under ambient air. The only noticeable change in spectral features is a slight narrowing of the emission from the OleylA sample after the first day (see Figure S5). PLQY values were measured over time (Fig. 4b). All samples exhibit a slight increase in PLQY in the first 50 hours. The exact reason for this effect is not clear, although it may be ascribed to passivation upon air exposure, as observed by others in lead iodide perovskites.[48] In all cases, after this initial increase, the PLQY remained constant up to 500 hours,
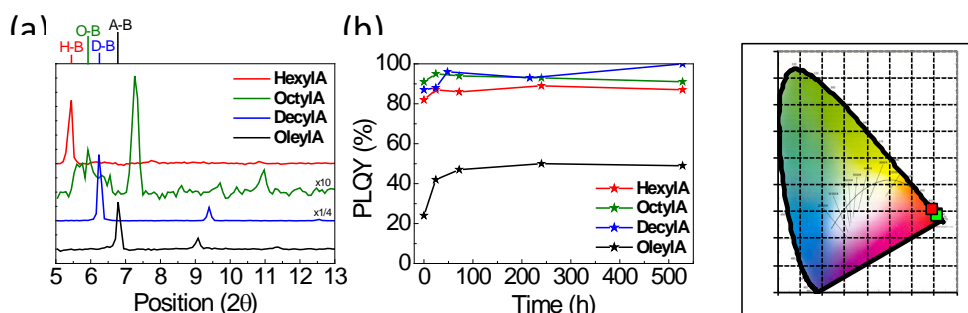

Fig. 4 (a) X-ray diffraction patterns of mixed Cs-MA NCs obtained with different alkylamines. (b) PLQY for suspensions of the same compounds monitored over time. (c) Corresponding CIE coordinates for the different samples.

demonstrating an excellent stability for iodide perovskite nanocrystals.[49] Furthermore, we note that replacing long-chain unsaturated oleylamine by shorter saturated alkylamines leads to a significant increase in absolute PLQY, with values that are close to unity. We speculate that this may be linked to a better quasi-2D crystal formation with less defects when rigid and straight spacer molecules are used.

Conclusions

In summary, we have presented a simple method to prepare efficient red-emitting hybrid quasi-2D perovskite nanocrystals of the type $(LA)_2(A)_{n-1}Pb_nI_{3n+1}$, where LA is an alkylamine and A a mixture of MA and Cs^+. We have discussed the effects of the synthesis conditions on the material structural and optical properties. In particular, we have shown that the PL can be tuned from the near-infrared to the visible by the alkyl chain length and that addition of butanol in the first washing step leads to improved purity of the sample with higher PLQY, exceeding 90%. The high PLQY is maintained for more than 500 h, making these materials especially promising for applications in light-emitting diodes and phosphors.

Acknowledgements

Conflicts of interest

There are no conflicts to declare.

Notes and references

1   L. Zhang, X. Zhou, X. Zhong, C. Cheng, Y. Tian and B. Xu, *Nano Energy*, 2019, **57**, 248–255.

2   F. Fu, T. Feurer, T. P. Weiss, S. Pisoni, E. Avancini, C. Andres, S. Buecheler and A. N. Tiwari, *Nat. Energy*, , DOI:10.1038/nenergy.2016.190.

3   W. S. Yang, B.-W. Park, E. H. Jung, N. J. Jeon, Y. C. Kim, D. U. Lee, S. S. Shin, J. Seo, E. K. Kim, J. H. Noh and S. Il Seok, *Science (80-.).*, 2017, **356**, 1376–1379.

4   Y. H. Kim, H. Cho, J. H. Heo, T.-S. Kim, N. Myoung, C. L. Lee, S. H. Im and T.-W. Lee, *Adv. Mater.*, 2015, **27**, 1248–1254.

5   X. Yang, X. Zhang, J. Deng, Z. Chu, Q. Jiang, J. Meng, P. Wang, L. Zhang, Z. Yin and J. You, *Nat. Commun.*, , DOI:10.1038/s41467-018-02978-7.

6   Q. A. Akkerman, L. Martínez-Sarti, L. Goldoni, M. Imran, D. Baranov, H. J. Bolink, F. Palazon and L. Manna, *Chem. Mater.*, 2018, **30**, 6915–6921.

7   H. Cho, S.-H. Jeong, M.-H. Park, Y.-H. Kim, C. Wolf, C.-L. Lee, J. H. Heo, A. Sadhanala, N. Myoung, S. Yoo, S. H. Im, R. H. Friend and T.-W. Lee, *Science (80-.).*, 2015, **350**, 1222.

8   K. Lin, J. Xing, L. N. Quan, F. P. G. de Arquer, X. Gong, J. Lu, L. Xie, W. Zhao, D. Zhang, C. Yan, W. Li, X. Liu, Y. Lu, J. Kirman, E. H. Sargent, Q. Xiong and Z. Wei, *Nature*, 2018, **562**, 245–248.

9   H. Wei, Y. Fang, P. Mulligan, W. Chuirazzi, H. H. Fang, C. Wang, B. R. Ecker, Y. Gao, M. A. Loi, L. Cao and J. Huang, *Nat. Photonics*, 2016, **10**, 333–339.

10   J. A. Steele, W. Pan, C. Martin, M. Keshavarz, E. Debroye, H. Yuan, S. Banerjee, E. Fron, D. Jonckheere, C. W. Kim, W. Baekelant, G. Niu, J. Tang, J. Vanacken, M. Van der Auweraer, J. Hofkens and M. B. J. Roeffaers, *Adv. Mater.*, , DOI:10.1002/adma.201804450.

11   H. Huang, L. Polavarapu, J. A. Sichert, A. S. Susha, A. S. Urban and A. L. Rogach, *NPG Asia Mater.*, 2016, **8**, e328–e328.

12   F. Zhang, H. Zhong, C. Chen, X. G. Wu, X. Hu, H. Huang, J. Han, B. Zou and Y. Dong, *ACS Nano*, 2015, **9**, 4533–4542.

13   Y. H. Kim, G. H. Lee, Y. T. Kim, C. Wolf, H. J. Yun, W. Kwon, C. G. Park and T. W. Lee, *Nano Energy*, 2017, **38**, 51–58.

14   A. Dutta, S. K. Dutta, S. Das Adhikari and N. Pradhan, *Angew. Chemie - Int. Ed.*, 2018, **57**, 9083–9087.

15   Y. H. Kim, C. Wolf, Y. T. Kim, H. Cho, W. Kwon, S. Do, A. Sadhanala, C. G. Park, S. W. Rhee, S. H. Im, R. H. Friend and T.-W. Lee, *ACS Nano*, 2017, **11**, 6586–6593.

16   L. C. Schmidt, A. Pertegás, S. González-Carrero, O. Malinkiewicz, S. Agouram, G. Mínguez Espallargas, H. J. Bolink, R. E. Galian and J. Pérez-Prieto, *J. Am. Chem. Soc.*, 2014, **136**, 850–853.

17   J. W. Lee, D. H. Kim, H. S. Kim, S. W. Seo, S. M. Cho and N. G. Park, *Adv. Energy Mater.*, , DOI:10.1002/aenm.201501310.

18   G. Niu, W. Li, J. Li, X. Liang and L. Wang, *RSC Adv.*, 2017, **7**, 17473–17479.

19   X. Liu, Z. Yang, C. C. Chueh, A. Rajagopal, S. T. Williams, Y. Sun and A. K. Y. Jen, *J. Mater. Chem. A*, 2016, **4**, 17939–17945.

20   A. Pan, B. He, X. Fan, Z. Liu, J. J. Urban, A. P. Alivisatos, L. He and Y. Liu, *ACS Nano*, 2016, **10**, 7943–7954.

21   J. Cho, Y. H. Choi, T. E. O'Loughlin, L. De Jesus and S. Banerjee, *Chem. Mater.*, 2016, **28**, 6909–6916.

22   H. Huang, J. Raith, S. V. Kershaw, S. Kalytchuk, O. Tomanec, L. Jing, A. S. Susha, R. Zboril and A. L. Rogach, *Nat. Commun.*, , DOI:10.1038/s41467-017-00929-2.

23   I. Levchuk, P. Herre, M. Brandl, A. Osvet, R. Hock, W. Peukert, P. Schweizer, E. Spiecker, M. Batentschuk and C. J. Brabec, *Chem. Commun.*, 2017, **53**, 244–247.

24   S. Sun, D. Yuan, Y. Xu, A. Wang and Z. Deng, *ACS Nano*, 2016, **10**, 3648–3657.

25   J. Shamsi, Z. Dang, P. Bianchini, C. Canale, F. Di Stasio, R. Brescia, M. Prato and L. Manna, *J. Am. Chem. Soc.*, 2016,

138, 7240–7243.

26 Z. Xiao, R. A. Kerner, N. Tran, L. Zhao, G. D. Scholes and B. P. Rand, *Adv. Funct. Mater.*, 2019, **1807284**, 1807284.

27 M. E. Kamminga, H. H. Fang, M. R. Filip, F. Giustino, J. Baas, G. R. Blake, M. A. Loi and T. T. M. Palstra, *Chem. Mater.*, 2016, **28**, 4554–4562.

28 Z. Wang, Q. Lin, F. P. Chmiel, N. Sakai, L. M. Herz and H. J. Snaith, *Nat. Energy*, 2017, **2**, 1–10.

29 C. C. Stoumpos, D. H. Cao, D. J. Clark, J. Young, J. M. Rondinelli, J. I. Jang, J. T. Hupp and M. G. Kanatzidis, *Chem. Mater.*, 2016, **28**, 2852–2867.

30 Y. Bekenstein, B. A. Koscher, S. W. Eaton, P. Yang and A. P. Alivisatos, *J. Am. Chem. Soc.*, 2015, **137**, 16008–16011.

31 K. Tanaka, T. Takahashi, T. Ban, T. Kondo, K. Uchida and N. Miura, *Solid State Commun.*, 2003, **127**, 619–623.

32 Z. Yang, A. Surrente, K. Galkowski, N. Bruyant, D. K. Maude, A. A. Haghighirad, H. J. Snaith, P. Plochocka and R. J. Nicholas, *J. Phys. Chem. Lett.*, 2017, **8**, 1851–1855.

33 X. Liang, R. W. Baker, K. Wu, W. Deng, D. Ferdani, P. S. Kubiak, F. Marken, L. Torrente-Murciano and P. J. Cameron, *React. Chem. Eng.*, 2018, **3**, 640–644.

34 D. H. Cao, C. C. Stoumpos, O. K. Farha, J. T. Hupp and M. G. Kanatzidis, *J. Am. Chem. Soc.*, 2015, **137**, 7843–7850.

35 G. Almeida, L. Goldoni, Q. Akkerman, Z. Dang, A. H. Khan, S. Marras, I. Moreels and L. Manna, *ACS Nano*, 2018, **12**, 1704–1711.

36 X. X. Zhang, C. Wang, Y. Zhang, X. X. Zhang, S. Wang, M. Lu, H. Cui, S. V. Kershaw, W. W. Yu and A. L. Rogach, *ACS Energy Lett.*, 2018, **4**, acsenergylett.8b02239.

37 S. Ahmad, C. Hanmandlu, P. K. Kanaujia and G. V. Prakash, *Opt. Mater. Express*, 2014, **4**, 1313–1323.

38 M. C. Weidman, M. Seitz, S. D. Stranks and W. A. Tisdale, *ACS Nano*, 2016, **10**, 7830–7839.

39 Y. H. Chang, J. C. Lin, Y. C. Chen, T. R. Kuo and D. Y. Wang, *Nanoscale Res. Lett.*, , DOI:10.1186/s11671-018-2664-5.

40 J. V. Milić, J. H. Im, D. J. Kubicki, A. Ummadisingu, J. Y. Seo, Y. Li, M. A. Ruiz-Preciado, M. I. Dar, S. M. Zakeeruddin, L. Emsley and M. Grätzel, *Adv. Energy Mater.*, 2019, **1900284**, 1–12.

41 D. N. Congreve, M. C. Weidman, M. Seitz, W. Paritmongkol, N. S. Dahod and W. A. Tisdale, *ACS Photonics*, 2017, **4**, 476–481.

42 Z. Yuan, Y. Shu, Y. Xin and B. Ma, *Chem. Commun.*, 2016, **52**, 3887–3890.

43 Y. Takeoka, K. Asai, M. Rikukawa and K. Sanui, *Bull. Chem. Soc. Jpn.*, 2006, **79**, 1607–1613.

44 N. Pradhan, D. Reifsnyder, R. Xie, J. Aldana and X. Peng, *J. Am. Chem. Soc.*, 2007, **129**, 9500–9509.

45 L. Yuan, R. Patterson, X. Wen, Z. Zhang, G. Conibeer and S. Huang, *J. Colloid Interface Sci.*, 2017, **504**, 586–592.

46 S. Gonzalez-Carrero, G. M. Espallargas, R. E. Galian and J. Pérez-Prieto, *J. Mater. Chem. A*, 2015, **3**, 14039–14045.

47 J. Yan, W. Qiu, G. Wu, P. Heremans and H. Chen, *J. Mater. Chem. A*, 2018, **6**, 11063–11077.

48 Y. Tian, M. Peter, E. Unger, M. Abdellah, K. Zheng, T. Pullerits, A. Yartsev, V. Sundström and I. G. Scheblykin, *Phys. Chem. Chem. Phys.*, 2015, **17**, 24978–24987.

49 B. Luo, S. B. Naghadeh and J. Z. Zhang, *ChemNanoMat*, 2017, **3**, 456–465.